Supporting online material, Yildiz et al. "1.5 nm localization in myosin V"

Materials and Methods

Sample Preparation of immobilized DNA samples. A Cy3 phosphoramadite dye (Amersham) was covalently attached to a DNA (5'Cy3-TGG-CGA-CGG-CAG-CGA-GGC-$(T)_{20}$-3', and hybridized to a complementary biotinylated strand 5'GCC-TCG-CTG-CCG-TCG-CCA-biotin-3'(gift of Tim Lohman, Washington Univ., St. Louis) (*1*). The double-stranded DNA was immobilized onto a glass coverslip (for objective-TIR) or onto a quartz slide (for prism-type TIR) via a streptavidin-BSA complex. The streptavidin-coated coverslip was made as follows. The coverslip was first cleaned by sonicating in 1M KOH solution and dried under nitrogen gas. 50 µL of 1 mg/ml BSA-biotin (A-8549 Sigma) in T50 buffer (10 mM Tris pH 8.0, 50 mM NaCl) was added to the coverslip via a laboratory-built flow-chamber, allowed to sit for ten minutes, and then washed with 100 µL of T50 buffer. 50 µL of 0.2 mg/ml Streptavidin (S-888 Molecular Probes) in T50 buffer was then added, allowed to sit for ten minutes, and then washed with 100 µL T50 buffer. 50 µL of 10 pM Cy3-DNA solution in T50 plus 1 mg/ml BSA (A-9085 Sigma) was then added, and the same washing procedure followed. The sample was washed with 100 µl of imaging buffer and sealed. Imaging buffer: 0.4% Glucose, 1% β-mercaptoethanol, 10 mM $MgCl_2$, 1% Gloxy {Gloxy = 1,665 units glucose oxidase, (G-7016, Sigma), ~26000 units Catalase (106810, Roche), in 100 µl T50 buffer, filtered with 0.2 µm syringe filters and centrifuged for 5 minutes at 13,000g}, in T50 buffer.

Myosin V labeling and actin immobilization. Calmodulin labeling with Bis-iodoacetamidorhodamine and exchange of the labeled calmodulin into myosin V has been described (*2, 3*). Labeling with Cy3 followed essentially the same procedure. Actin

immobilization via biotinylated actin (1 biotin/20 actin monomers) bound to a streptavidin-coated coverslip has also been described (*3*). Myosin V was then added to the sample flow chamber, excess myosin removed, and a solution containing ATP and imaging buffer was added. To ensure that F-actin was immobile, we also labeled F-actin with tetramethylrhodamine (TMR, gift of John Corrie) (1 TMR/1000 actin monomers) and biotin (1:20), and immobilized the labeled actin molecules on a streptavidin-coated coverslip. The surface was excited by TIRF and the emission was imaged onto a CCD camera. We first determined the traces of actin filaments and then selected TMR spots on the filament that were sparse enough to separate from each other. We determined that single TMR molecules on actin filaments were localized with very similar variance compared to immobilized dyes on a glass surface (data not shown), indicating that actin was highly immobile.

Total Internal Reflection Fluorescence Microscope. Single Cy3-DNA and BR- (Cy3-) labeled Myosin V images were observed by objective type- TIRF using an Olympus IX70 epifluorescence microscope and a 60X objective (Olympus, NA=1.45, oil). Prism-type TIRF was also used for the control DNA experiments with similar results although with slightly wider PSFs and lower collection efficiency due to the lower numerical aperture (Olympus, NA=1.2, water). Linearly polarized 532 nm laser light (CrystaLaser NdYAG, model #GCL-075-L, 75 mW) was passed through a half-wave plate (CVI Laser), and a polarizing beam splitter cube (Karl Lambrecht), which split the laser light into two optical pathways for objective- and prism-type TIR. For objective-type TIRF, the laser light was expanded by a 5X beam expander and focused by a 50 cm focal-length, 2”-diameter, lens into the back focal plane of the objective. For prism-type TIRF, the laser light was focused by 5 cm focal length lens through a suprasil pellin broca prism (CVI Laser) onto the sample. The power at the sample was 2 mW to 5 mW in objective-

type TIRF, illuminating a circle of ~ 40 μm diameter. For prism type TIRF, the power at the sample could not be measured; the incident laser power at the prism was 30 mW and the spot size was ~50 μm x 100 μm. The fluorescent photons were passed through a Cy3 filter set (HQ585/70, 545DRLP, Chroma), externally magnified by a 2.5X eyepiece (Olympus) and detected by a back thinned, frame-transfer CCD (Micromax 512BFT, Roper Scientific, 512 X 512 X 13 μm pixels). At 150 x magnification, the effective pixel size is 86 nm (*a* in Eq'n. 1). The camera can acquire a full frame in 0.35 sec without significant dead time at 1 MHz readout rate, with 8 electrons per pixel readout noise, and <10 electrons/pixel/sec dark current at -45°C. By using only part of the CCD, the frame rate can be increased further, and we have successfully measured high quality PSFs at 0.2-second time resolution. Using a high quantum efficiency, low noise CCD was essential to achieve the high signal to noise (~30) and spatial localization. An intensified CCD, which is commonly used, leads to significantly poorer signal-to-noise and localization.

To translate the sample in a stepwise fashion in TIRF, a nanometric stage (Mad City Labs: NanoH-70/invar, with 0.7 nm position accuracy, used in closed loop scanning mode) was moved unidirectionally in user-defined steps, in approximately 8, 12, or 30 nm increments. The nanostage was bolted to the mechanical stage of the microscope, enabling large-scale motion as needed. Moving the mechanical stage to a new area on the sample caused a drift that decayed exponentially in time. Hence we waited two minutes after moving the mechanical stage before acquiring data.

The number of steps/sec produced by the nanometric stage was user-controllable via software and made either fixed (typically one step per four seconds) or Poisson-distributed (average of one step per four seconds). The timing of the steps was recorded in software.

Synchronization of the scanner, shutter, detectors and the acquisition program was done by a computer board (PCI-DIO-96, National Instruments) and controlled by a laboratory-written program in C++.

Data Analysis & Spatial Localization: A well-optimized diffraction-limited spot forms an Airy disk (*4*). We fit our images to a 2-D Gaussian function, which is very similar to the zeroth order diffraction peak of an Airy pattern. The Gaussian function is defined as

$$P_G(x, y; z_0, A, x_0, y_0, s_x, s_y) = z_0 + A\exp\left[-\frac{1}{2}\left[\left(\frac{(x-x_0)}{s_x}\right)^2 + \left(\frac{(y-y_0)}{s_y}\right)^2\right]\right] \quad \text{(S1)}$$

z_0 is a constant term due to background fluorescence, detector noise, and a constant (noiseless) CCD offset. A is the amplitude, x_0 and y_0 are the coordinates of the center, and s_x and s_y are standard deviations of the distribution in each direction.

We fit our images to Eq. (S1) by minimizing least squares via a user-defined program in SigmaPlot 8.0 (SPSS Inc.). Consecutive images were also fit automatically by a laboratory-written program in IDL 5.5 (Research Systems Inc.). The two programs yielded identical results and the σ_μ's were consistent with Eq. 1.

Data Analysis of Step Sizes for 1-d stepping via nanometric stage. We changed the position of immobilized Cy3 labeled DNA molecules by moving a nanometric stage in user-defined steps and rates. Each CCD image contained many single molecules. For analysis, each single molecule was chosen by hand and an 11 x 11 pixel image surrounding the molecule was analyzed via an IDL-based program. At an imaging rate of 2 frames/sec and a stepping rate at a constant 4 seconds per step, 8 images of the fluorophore were collected between steps. For a Poisson distributed step rate, the time between steps is variable. The step size was determined by

comparing the average position immediately before and after the step. The time of the step was determined visually from the trace of the PSF centers when the position took a sudden change, and this time was correlated to the output of the stage. If a step occurred during acquisition of one image, an intermediate position was found.

To quantitatively determine the step size we did the following calculations:

1. The average position (μ_i), standard deviation (σ_i), and standard error of the mean ($\sigma_{\mu_i} = \sigma_i / N_i^{1/2}$), of the multiple images before (*i*th position) and after (*i*+1 position) the step(s) are calculated. N_i is the number of images at the i^{th} position.
2. The step size, $d_i = \mu_{i+1} - \mu_i$ is determined.
3. The standard deviation, σ_{d_i}, of step i is calculated using error propagation:

$$\sigma_{d_i}^2 = \sigma_{\mu_{i+1}}^2 + \sigma_{\mu_i}^2 + \sigma_{st}^2$$

where σ_{st} is the standard deviation (~0.7 nm) of the piezo stage. Note that each step will have somewhat different uncertainty (standard deviation) due to slight variability in photons collected per image, and more significantly, due to the different number of images between steps in the Poisson distributed case.

4. The average step size (μ_d) and standard deviation of the average step size (σ_{μ_d}) are calculated by averaging d_i, weighted by their individual uncertainties (σ_{d_i}):

$$\mu_d = \frac{\Sigma_i \left(d_i / \sigma_{d_i}^2 \right)}{\Sigma_i \left(1 / \sigma_{d_i}^2 \right)} \qquad \sigma_{\mu_d}^2 = 1 \Big/ \Sigma_i \left(1 / \sigma_{d_i}^2 \right)$$

μ_d and σ_{μ_d} are the values shown in Fig. 2. To determine the accuracy of the average step size(s), we then compared μ_d to the expected step sizes based on the calibrated stage motion.

In order to determine absolute distances and step sizes, the effective pixel size was measured and the stage calibrated. The pixel size was determined by imaging a 5000g/in reticle. The 86.1 nm pixel size was in excellent agreement with the expected value of 86.7 nm based on the actual pixel size of 13 μm and 150x magnification. To calibrate the stage, we made several measurements. We made large steps (e.g. 100-200 nm steps) imaging beads or single molecules and measured the distance from the center of the PSFs and compared this to the expected step size based on the voltage of the stage (10V/70μm). The agreement was better than 1%. We then made a series of many small steps (e.g. 6 nm, 12 nm, 30 nm…) using single molecules and beads that lasted several minutes. We then determined the total distance by measuring the distance between the centers of the initial and final PSFs, and determined the step size by dividing this distance by the total number of steps. This procedure was repeated on > 20 molecules with each molecule yielding > 15 steps. The measured step size agreed with the expected step size based on the stage voltage to within +/- 0.2 nm. The linearity of the stage was also tested by taking > 100 steps of step-size ranging from 4 nm to 200 nm and comparing the expected total distance based on voltage calibration to that measured by the PSFs of beads. The linearity was excellent, >0.998.

Data Analysis of Step Sizes for MyoV stepping in 2-D. The following is a two-dimensional generalization for step size analysis described above. To determine step size and its uncertainty: The average position $(\bar{x}_i, \bar{y}_i)$, standard deviation $(\sigma_{x_i}, \sigma_{y_i})$, and standard error of the mean

($\sigma_{\bar{x}_i}, \sigma_{\bar{y}_i}$) where $\sigma^2_{\bar{x}_i} = \sigma^2_{x_i} / N_i$, of the multiple images before (*i*th position) and after (*i*+1 position) the step(s) are calculated in x and y directions. N_i is the number of images at the i^{th} position.

1. The distance between mean positions of *i*th and *i+1* positions ($\Delta x_i, \Delta y_i$) in each direction are calculated. $\Delta x_i = \bar{x}_{i+1} - \bar{x}_i$, $\Delta y_i = \bar{y}_{i+1} - \bar{y}_i$.
2. The standard deviation of ($\Delta x_i, \Delta y_i$) are calculated by error propagation:

$$\sigma^2_{\Delta x_i} = \sigma^2_{\bar{x}_{i+1}} + \sigma^2_{\bar{x}_i} \quad , \quad \sigma^2_{\Delta y_i} = \sigma^2_{\bar{y}_{i+1}} + \sigma^2_{\bar{y}_i}$$

3. Each step size (d_i) and its standard deviation (σ_{d_i}) are calculated by Pythagorean theorem and error propagation, respectively:

$d_i = f(x, y) = \sqrt{\left((\Delta x)^2 + (\Delta y)^2\right)}$ where *d* is the step size

$$\sigma^2_{d_i} = \left(\frac{\partial f}{\partial \Delta x}\right)^2 \cdot \sigma^2_{\Delta x} + \left(\frac{\partial f}{\partial \Delta y}\right)^2 \cdot \sigma^2_{\Delta y} = \frac{(\Delta x)^2}{\left((\Delta x)^2 + (\Delta y)^2\right)} \cdot \sigma^2_{\Delta x} + \frac{(\Delta y)^2}{\left((\Delta x)^2 + (\Delta y)^2\right)} \cdot \sigma^2_{\Delta y}$$

SUPPORTING ON-LINE RESULTS

Photostability and Gaussian Curve-fitting to a Point Spread Function. Fig. S1 shows the intensity (photon counts in pixel of maximum intensity) vs. time for the PSF shown in Fig 2b. The dye lasts for 50 seconds, emitting ~1.4 million collected photons before it suddenly photobleaches. This photostability is typical in our experiments. For example, in one representative image sequence containing 300 individual molecules, three-quarters of the molecules emitted more than 2 million total collected photons with a few emitting 5 million collected photons, and 2/3 of the molecules lasting more than 2 minutes when data acquisition was stopped. The collection efficiency of the microscope was not measured, and hence we cannot determine the total number of emitted photons.

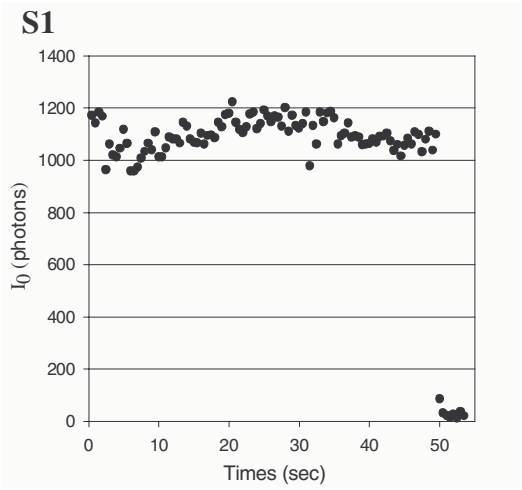

Fig. S1. Intensity vs.time for point spread function in Fig. 2b. Each point represents the intensity of the peak pixel in a 0.5 sec. image.

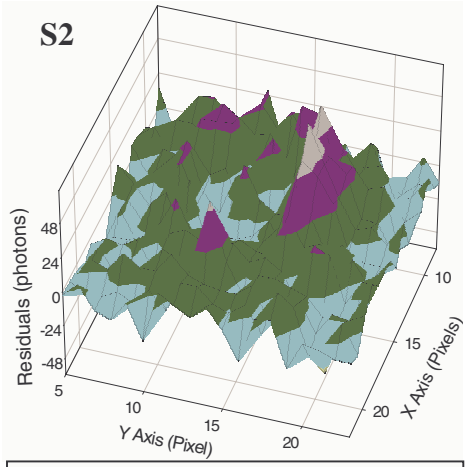

Residuals of the difference between the Gaussian curve-fit and the point spread function shown in Fig. 2b.

Fig. S2 shows the residuals of the Gaussian curve fit to the PSF in Fig. 2b. The slight ring (purple) is due to the difference between a Gaussian function and an Airy pattern. The fit is excellent (r2 = 0.994) but this systematic error causes the reduced χ^2_r to be greater than 1 ($\chi^2_r = 1.48$).

74 nm steps. A video showing the movement of the point-spread-function as a function of time for the 74 nm lower-right trace of Fig. 3 is available online.

12 nm steps. In addition to the ~30 nm and ~8 nm steps shown in Fig. 2, we also measured ~12 nm steps, as shown below.

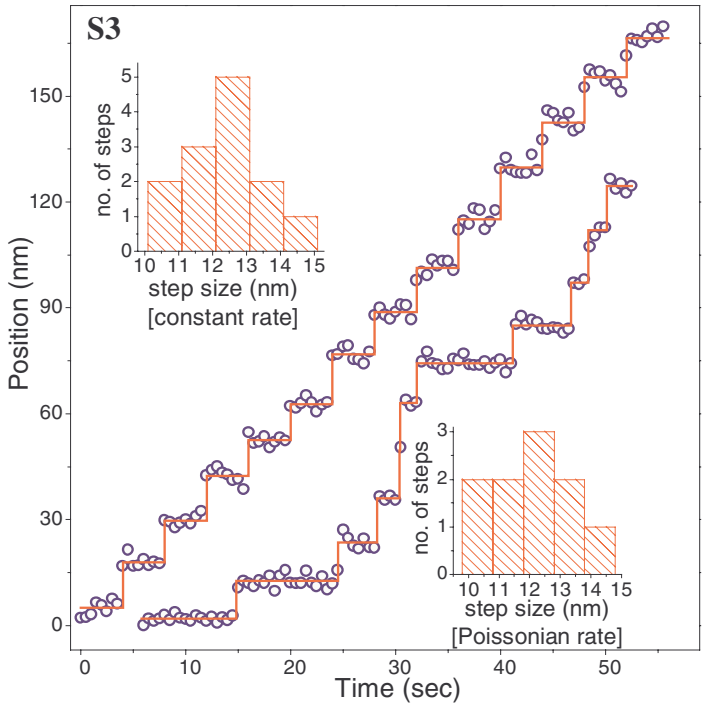

References

1. T. Ha *et al.*, *Nature* **419**, 638 (2002).
2. T. Sakamoto, I. Amitani, E. Yokota, T. Ando, *Biochem Biophys Res Commun* **272**, 586 (2000).
3. J. N. Forkey, M. E. Quinlan, M. Alexander Shaw, J. E. Corrie, Y. E. Goldman, *Nature* **422**, 399 (2003).
4. Hecht, *Optics* (Addison Wesley, San Francisco, ed. 4th, 2002).